

# Achieving very low mercury levels in refinery wastewater by membrane filtration

Meltem Urgun-Demirtas<sup>a</sup>, Paul L. Benda<sup>a</sup>, Patricia S. Gillenwater<sup>a</sup>, M. Cristina Negri<sup>a,\*</sup>, Hui Xiong<sup>b</sup>, Seth W. Snyder<sup>a</sup>

<sup>a</sup> Argonne National Laboratory, Energy Systems Division, 9700 S. Cass Avenue, Argonne, IL 60439, United States

<sup>b</sup> Argonne National Laboratory, Center for Nanoscale Materials, 9700 S. Cass Avenue, Argonne, IL 60439, United States

## ARTICLE INFO

### Article history:

Received 12 October 2011

Received in revised form 13 February 2012

Accepted 15 February 2012

Available online 22 February 2012

### Keywords:

Refinery wastewater

Mercury

Membrane filtration

Great Lakes Initiative mercury criterion

## ABSTRACT

Microfiltration (MF), ultrafiltration (UF), nanofiltration (NF) and reverse osmosis (RO) membranes were evaluated for their ability to achieve the world's most stringent Hg discharge criterion (<1.3 ng/L) in an oil refinery's wastewater. The membrane processes were operated at three different pressures to demonstrate the potential for each membrane technology to achieve the targeted effluent mercury concentrations. The presence of mercury in the particulate form in the refinery wastewater makes the use of MF and UF membrane technologies more attractive in achieving very low mercury levels in the treated wastewater. Both NF and RO were also able to meet the target mercury concentration at lower operating pressures (20.7 bar). However, higher operating pressures ( $\geq 34.5$  bar) had a significant effect on NF and RO flux and fouling rates, as well as on permeate quality. SEM images of the membranes showed that pore blockage and narrowing were the dominant fouling mechanisms for the MF membrane while surface coverage was the dominant fouling mechanism for the other membranes. The correlation between mercury concentration and particle size distribution was also investigated to understand mercury removal mechanisms by membrane filtration. The mean particle diameter decreased with filtration from  $1.1 \pm 0.0 \mu\text{m}$  to  $0.74 \pm 0.2 \mu\text{m}$  after UF.

© 2012 Elsevier B.V. All rights reserved.

## 1. Introduction

Mercury is currently one of the thirteen metals on the US EPA's priority pollutants list [1]. The fate of mercury in the environment is complex because of its persistence, biotransformation into methyl mercury, bioaccumulation and biomagnification in aquatic food webs [2]. The removal of mercury at point source discharges is crucial to minimize the entrance of mercury into watersheds and its subsequent biotransformation into methyl mercury.

The Great Lakes Initiative ("a combined effort between the United States and Canada to help restore, maintain, and protect the ecosystem of the Great Lakes Basin") (GLI) established a water quality criterion for mercury (<1.3 ng/L or parts-per-trillion or ppt) [3]. This criterion is the world's most stringent surface water discharge limit for Hg. Many states in the USA have been currently implementing this criterion and issuing Hg permit limits in the 1–10 ng/L range. Therefore, the removal of mercury from a variety of industrial wastewaters such as refineries, coal-fired power plants, mining, chloralkali plants with the Hg-cell process as well as from municipal wastewaters is becoming necessary to meet National Pollutant Discharge Elimination System (NPDES) requirements for surface water discharge in some parts of the USA. As limits

become more restrictive, many dischargers in the Great Lakes area are developing plans to meet these new limits. However, designing treatment processes to achieve this purpose is not an easy task because of uncertainties about the ability of existing technologies to achieve low-ng/L levels in treated wastewater [4].

Many of the traditional wastewater treatment processes including precipitation, ion exchange, and adsorption are effective when the mercury is in the soluble and ionic forms. These methods may not be effective when the Hg is in the particulate/colloidal form. However, mercury in many wastewaters is typically strongly associated with particles in the effluent stream [4]. The affinity of mercury for particulates makes the use of membrane technology attractive in achieving low-ng Hg/L levels in the treated effluent.

The objective of this treatability study was to investigate the potential of filtration to treat an oil refinery effluent and to determine its ability to meet the targeted effluent limits (mercury <1.3 ng/L) at the bench-scale. A series of tests was conducted to assess the effectiveness of microfiltration (MF), ultrafiltration (UF), nanofiltration (NF), and reverse osmosis (RO) membranes in providing effluent at or below the target mercury concentration.

The bench-scale treatability tests were designed to address the following goals:

1. Determine the capability of different membrane filtration technologies to achieve the targeted mercury concentration

\* Corresponding author. Tel.: +1 630 252 9662; fax: +1 630 252 4130.  
E-mail address: [negri@anl.gov](mailto:negri@anl.gov) (M.C. Negri).

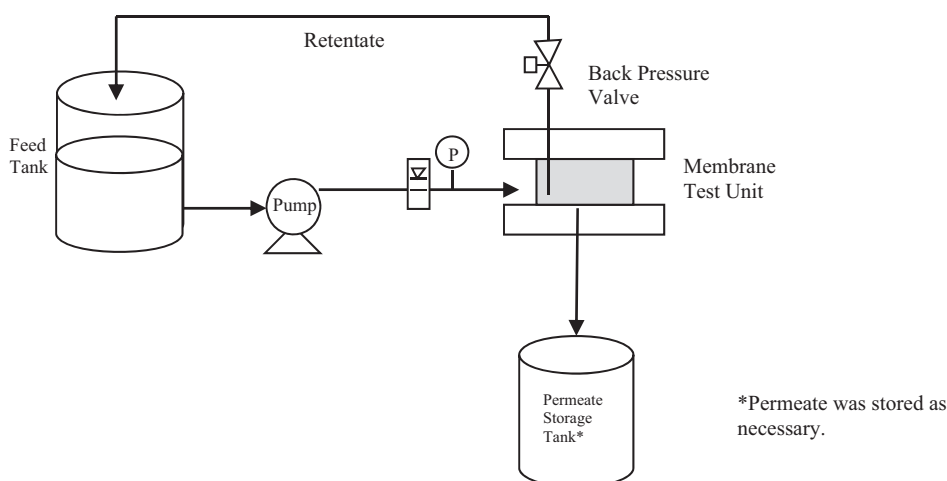


Fig. 1. Flow diagram of the bench-scale membrane test unit.

(<1.3 ng/L) in the “as-is” effluent (i.e. without any pretreatment or prefiltration);

2. Simulate the flow dynamics within a full-scale membrane unit by using a bench-scale membrane unit to evaluate the membrane filter characteristics, such as fouling, as well as to determine particle size distribution in the refinery wastewater before and after membrane operations.
3. Investigate systematically the flux and rejection properties of the tested membranes as a function of pressure.

## 2. Materials and methods

### 2.1. Testing equipment and materials

The filtration test was performed in a lab-scale cross flow membrane filtration cell (CF 042, Sterlitech, California) (Fig. 1) [5,6]. This cell can be used in a variety of membrane filtration applications. The cell body is made of Delrin® acetal. The top and bottom plates are made of stainless steel to accommodate pressures up to 69 bar.

Table 1 shows the properties of the 42 cm<sup>2</sup> flat sheet membranes used in these experiments. The equipment and flat sheet membranes were cleaned before testing, according to the vendor's instructions [5].

### 2.2. Wastewater samples

The treatability test was conducted on effluent taken from the secondary clarifier of an oil refinery (CE). The CE samples were tested in several different batches, with each batch equal to the amount that would be used with a negligible change in mercury speciation and composition within a 1 week time period based on previous work [7]. An independent EPA certified analytical laboratory (Lab A) collected wastewater samples at the source and delivered them to Argonne using “clean hands-dirty hands” procedures required by US EPA Method 1669 for low level metal analysis [8,9].

### 2.3. Experimental procedure

The CE was delivered to the membrane unit from the feed tank with a volumetric pump while a rotameter was used to measure feed flow rate (Fig. 1). Next, pressurized CE was exposed to the membrane. The permeate stream was collected into an acid-clean glass container [8] to determine the permeate ( $J_v$ ) flow rate, as well as to analyze its characteristics, including mercury concentration,

turbidity and pH. The permeate flow rate was measured with a graduated cylinder and stopwatch. The membrane type and operating conditions were selected based upon literature review and manufacturers' suggestions [5,10–16]. The focus of this testing was to evaluate the permeate quality when treating CE with different membrane types.

The feed and permeate flow rates were measured during the experiments to calculate the system recovery, which is defined as the ratio of permeate flow to feed flow. The permeate rate measurements were also used to calculate the flux of each tested membrane type under varying operating pressures (Table 2). Once the system reached each of the required operating pressures, the permeate sample was collected after 30 min of filtration which has been reported to be sufficient to reach constant permeate flux and rejection with pressure-driven membranes [10,11]. All four membrane units were operated at a constant feed flow rate of 2.5 L/min in order to obtain the permeate required for analysis of treated wastewater in a short period of time (1–3 h).

Before the experiments with CE, initial runs were conducted with MilliQ water (18 M $\Omega$  cm<sup>-1</sup> resistivity) to assess, minimize and eliminate any mercury contamination from the equipment (equipment blank), as well as to determine the clean membrane flux at the specified pressure range, as noted in Table 3. The initial screening experiments were performed with CE “as-is” samples. The focused tests were performed with CE that had been filtered through 5  $\mu$ m, 1  $\mu$ m, and 0.45  $\mu$ m in-line-filters (Millipore GWSC5001 and GWSC10001, and Whatman Polycap GW 6714-6004). The sequential filtration was done to enable the membrane filtration unit to run stably and successfully, since in many membrane applications one membrane process is typically followed by another for the purpose of producing high-purity water and decreasing operational problems [4]. The experimental layout for the focused testing is shown in Fig. 2 [4,18].

All testing was conducted in a Class 100 clean room facility following the guidelines in US EPA Method 1631E for low level mercury measurements [9].

### 2.4. Analyses

The samples were collected into clean sample bottles provided by the certified lab as described in EPA Method 1631E [9]. The CE<sub>t=0</sub>, permeate, and retentate samples were collected and analyzed for mercury to determine the removal percentage for each tested membrane. Samples were sent to EPA certified independent Lab B for analysis of the total and dissolved mercury by EPA Method

**Table 1**  
Characteristics of membrane filters used for mercury removal.

Filtration type/manufacturer	Membrane specifications			Operating conditions Pressure (bar)	References
	Polymer	Pore size	Designation		
Microfiltration/GE Osmonics	PVDF	0.3 $\mu\text{m}$	JX	1.01, 2.1	5, 14, 15
Ultrafiltration/Koch	Polysulfone	0.003 $\mu\text{m}$	HFK-131	1.01, 2.1, 5.2	5, 10, 14
Nanofiltration/GE Osmonics	Thin film	0 MWCO	DK	1.4, 4.8, 10.3	5, 11–16
RO/GE Osmonics	Polyamide	0 MWCO	AD	3.4, 13.8, 55.2	5, 13, 16

**Table 2**  
Operating conditions for screening and focused experiments.

Filtration type/manufacturer	Operating conditions pressure (bar)		
	Planned	Tested	
		Screening	Focused
Microfiltration GE Osmonics	1.01, 2.1	1.01, 2.8, 4.1	2.8
Ultrafiltration Koch	1.01, 2.1, 5.2	3.4, 5.0	3.4, 6.9
Nanofiltration GE Osmonics	1.4, 4.8, 10.3	20.7, 34.5, 48.3	Not applicable
RO GE Osmonics	3.4, 13.8, 55.2	20.7, 34.5, 48.3	Not applicable

**Table 3**  
Typical product recovery and flux values for different membrane applications compared with experimental results.

Membrane	Influent	Pressure (bar)	Reported flux <sup>a</sup> (L/(m <sup>2</sup> h))	Initial flux (L/(m <sup>2</sup> h))	% Reduction in initial flux	% Recovery rate <sub>initial</sub>	Reported % product recovery (13)
Microfiltration	MilliQ	2.8	221 @ 2.1 bar	38	70%	35	94
	CE	2.8		11			–98
Ultrafiltration	MilliQ	3.4	781 @ 3.4 bar	34	73%	30	70
	CE	3.4		9			–80
RO	MilliQ	20.7	25 @ 55.1 bar	39	85%	56	
	CE	20.7		6		20	70
	CE	34.5		196		45	–85
	CE	48.3		12		87	
Nanofiltration	MilliQ	20.7	37 @ 6.9 bar	29	55%	49	
	CE	20.7		13		31	80
	CE	34.5				41	–85
	CE	48.3				51	

<sup>a</sup> Manufacturers' reported flux (5).

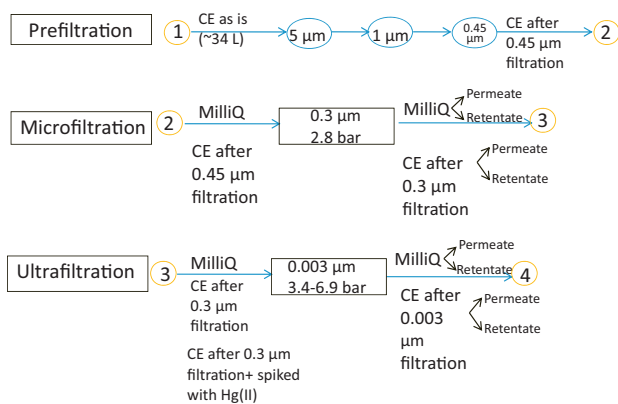


**Fig. 2.** Experimental layout for focused testing.

1631 E [9] within 24 h. The samples were preserved and analyzed for Hg by the analytical lab according to the EPA Method 1631E. Samples were also sent to a different, specialized lab (Lab C) for particle size and size distribution analysis [17] by light obscuration and dynamic light scattering method.

The UF and MF membranes were also analyzed to determine the fate of mercury during the filtration. Membrane filters were first submerged in a 50% BrCl solution for 6 h at 50 °C. This digestion method pulls any mercury that is adsorbed to the filter into

solution. Then, the solution was analyzed by Method 1631E for Hg [9]. The MDL of this analysis was 0.1 ng per filter.

Scanning Electron Microscopy (SEM) analysis was performed to obtain micrographs of clean and used (fouled) membrane filters. A conductive Au layer was coated on the samples prior to SEM by a sputter coater (Emitech K675X, Kent, UK). SEM images were recorded with a JSM-7500F Field Emission SEM (JEOL Ltd., Tokyo, Japan) at 30 kV accelerating voltage.

### 3. Results and discussion

Experiments were performed with relatively high volumes of water (19–34 L) to maintain a constant mercury concentration within the system and to identify any mercury loss or contamination during the experiments. This procedure was used because of the low mercury concentration in the CE, as well as the challenges and analytical restrictions encountered when measuring low ng/L levels in water samples [9]. In addition, the membrane unit was also operated in batch-mode to maintain a relatively constant mercury concentration within the system. The only losses from the system were samples removed for analysis. The work for this study was separated into two phases:

#### 3.1. Screening experiments

Phase I consisted of initial screening experiments to determine which membrane filtration process(es) would be suitable for the

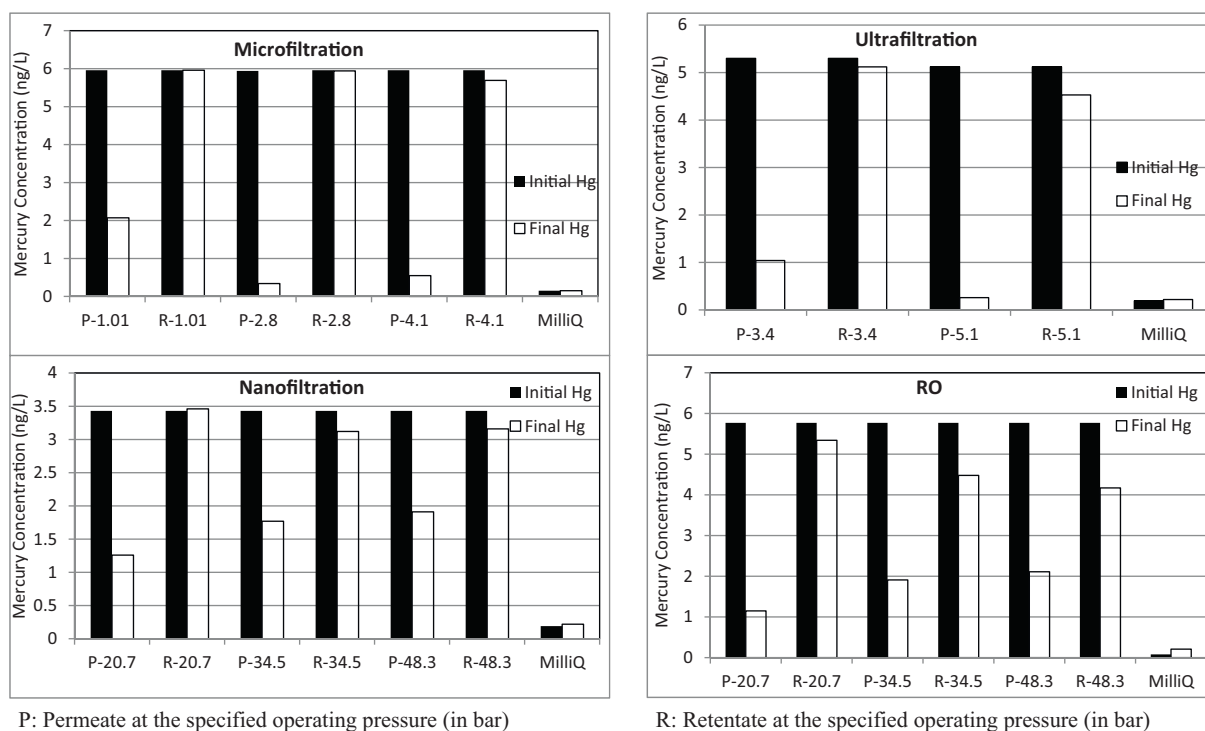


Fig. 3. Inlet and effluent characteristics and performance summary for membrane filtration.

refinery's wastewater characteristics and would also allow stringent mercury levels to be met in the treated wastewater. The objective of this testing was to evaluate the permeate quality when treating the CE with different membrane types. The best operating condition for each type of membrane was determined as a function of the operating pressure. The performance of each membrane technology was compared in terms of its ability to meet targeted effluent limits in the treated CE. Important preliminary performance parameters, such as permeate flux and system recovery, were also identified for each tested membrane type under varying operating pressures, as described in Table 3. Since the experiments were performed with CE "as-is" with no pretreatment, the tested operating pressure values were much higher than the planned operating pressures (Table 2) because of the fouling characteristics of the CE which are discussed later.

Initial experiments were performed with MilliQ water ( $18\text{ M}\Omega\text{ cm}^{-1}$  resistivity) not only to determine the clean membrane flux at the pressure range specified in Table 2, but also to assess mercury contamination (equipment blank). The manufacturer's reported flux values were also higher than that of the data obtained from the MilliQ run, except for the RO filters. It should be noted that the manufacturer's reported data did not include information on the characteristics of the water that they tested [5]. The CE water flux for each tested membrane was considerably lower than that of the MilliQ water flux (Table 3). The comparison of both flux data is important to understand the fouling characteristics of the CE.

Operating conditions and water quality data for the tested membrane technologies are summarized in Fig. 3. The retentate stream was also analyzed for mercury to identify any contamination (gain) or loss during operation of the membrane unit (method blank). The Hg concentration in the retentate samples (Fig. 3) was basically the same as that of the initial  $t=0$  samples. This is because the equipment and method blanks showed no Hg contamination or losses during membrane operation. Another contributing factor was that the membranes were operated with high volumes of wastewater (18.9 L ~ 5 gal) in batch-mode.

Achieving the  $<1.3\text{ ng Hg/L}$  target in the treated water was the most significant criteria of success in these membrane filtration experiments. The MF and UF processes were very successful in achieving the required discharge criteria for mercury (Fig. 3).

Both NF and RO were also able to meet the target mercury concentration when operated at lower pressures (20.7 bar) (Fig. 3). The NF and RO flux decline and fouling rates as well as deterioration of permeate quality increased significantly with an increase in pressure. This finding also has been reported by Zhu and Elimelech [22]. Shibutani et al. (2011) described the significant flux decline as a result of lower foulant rejection at the membranes where more foulant can penetrate and could adsorb and/or deposit on the surface [23].

High membrane operating pressures (20.7–48.3 bar) lead to high convective flow on the membrane surface and high initial permeate flux rates and rapid accumulation of solids on the membrane surface. The membrane surface characteristics might change presumably due to concentration polarization, adsorption of particulates on the membrane surface, and electrostatic effects [24–28]. The rapid solids accumulation and concentration polarization on the membrane surface has been shown to hinder the membrane permeability [22].

No pressure drop occurred during the operation of the membranes that would suggest membrane breakage; the pressure was very stable throughout the experiments. Also, no water leakage was observed from the system—the volume of water at the beginning of the experiments was the same as the sum of the volumes of collected samples and retentates. Based on these observations, it was concluded that low permeate quality was not caused by membrane failure, but presumably was related to the fouling characteristics of the tested CE water. From the particle size analysis of the CE "as-is" samples provided in Table 4, it can be seen that the mean particle size is  $1.1\text{ }\mu\text{m}$  and that 90% of the particles are  $<1.2\text{ }\mu\text{m}$ . Therefore, it can be concluded that the CE, which had ~1000 ppm of dissolved solids and an average of 15 ppm of TOC [7], contained high concentrations of colloidal particles ranging from a few nanometers to a few micrometers. Winfield [19] reported that dissolved colloidal

**Table 4**  
Particle size analysis by Accusizer (by number and volume).<sup>a</sup>

Sample	Arithmetic mean	Mode	Median	Number-based percentiles less than indicated size ( $\mu\text{m}$ )			
				10%	50%	90%	95%
CE as-is	1.1 $\pm$ 0.0	0.60 $\pm$ 0.0	0.67 $\pm$ 0.0	0.54 $\pm$ 0.0	0.67 $\pm$ 0.0	1.2 $\pm$ 0.1	1.7 $\pm$ 0.2
CE after 0.3 $\mu\text{m}$	1.01 $\pm$ 0.1	0.54 $\pm$ 0.0	0.65 $\pm$ 0.0	0.53 $\pm$ 0.0	0.65 $\pm$ 0.0	1.2 $\pm$ 0.1	1.86 $\pm$ 0.3
CE after 0.003 $\mu\text{m}$	0.74 $\pm$ 0.2	0.56 $\pm$ 0.0	0.62 $\pm$ 0.04	0.54 $\pm$ 0.0	0.62 $\pm$ 0.0	0.85 $\pm$ 0.3	1.05 $\pm$ 0.6
Sample	Arithmetic mean	Mode	Median	Volume-based percentiles less than indicated size ( $\mu\text{m}$ )			
				10%	50%	90%	95%
CE as-is	35.1 $\pm$ 0.3	33.9 $\pm$ 16.1	29.5 $\pm$ 2.2	13.1 $\pm$ 0.0	29.5 $\pm$ 2.2	66.2 $\pm$ 5.0	80.1 $\pm$ 9.1
CE after 0.3 $\mu\text{m}$	39.0 $\pm$ 4.0	43.0 $\pm$ 2.3	38.7 $\pm$ 3.5	19.8 $\pm$ 5.8	38.7 $\pm$ 3.5	57.5 $\pm$ 6.3	63.6 $\pm$ 6.5
CE after 0.003 $\mu\text{m}$	38.9 $\pm$ 1.5	42.3 $\pm$ 1.3	38.5 $\pm$ 0	20.9 $\pm$ 1.3	38.5 $\pm$ 0.0	58.3 $\pm$ 3.7	62.2 $\pm$ 4.1

<sup>a</sup> Experiments were performed with triplicate samples.

materials ( $<5 \mu\text{m}$ ) in secondary effluent wastewater contributed significantly to RO membrane fouling. Severe fouling was observed when the small colloids (75 nm) were present along with natural organic matter and salts in the surface water [18,20]. In this current study, the RO and NF membranes were fed CE potentially containing a high concentration of colloidal particles, which most likely contributed to the observed fouling.

Moreover, operation of the membranes at high pressures apparently created a shear field on the membrane surface, which most likely impacted the particle size distribution of the CE water and the detachment/attachment pattern of particles on the membrane surface. Furthermore, there is also the possibility that operation of membranes at high pressures might impact particle morphology [21,22]. In this study, high operating pressure also probably resulted in aggregate break-up in the wastewater, which may have caused the particle-associated mercury to detach from the particles and become dissolved. The accumulation of dissolved mercury on the membrane surface, as well as the subsequent release into the permeate produced higher mercury concentrations in the permeate than expected. It should be noted that dissolved mercury ( $M_w = 200 \text{ g/mole}$ ) is small enough to pass through the RO and NF membranes. This might explain the high mercury concentrations in the six samples collected after operation of the RO and NF membrane filters. Similar test results have been reported by Schafer et al. (2009) [20]. A similar impact of fouling on permeate quality also has been shown to occur with organic compounds, such as plastic additives ( $M_w = 78\text{--}266 \text{ g/mole}$ ) and endocrine disruptors such as hormones, pharmaceutical compounds, and humic acids ( $\sim 100 \text{ kDa}$ ) [24,25,27]. Additionally, other organics, such as sodium alginate-polysaccharide ( $>100 \text{ kDa}$ ), disinfection by-products, and inorganic colloidal materials (silica colloids, iron oxide), have similarly caused fouling and impacted permeate quality [21,22,26]. Sioutopoulos et al. [21] reported that the presence of a complicated shear field during the RO operation will most likely affect the size distribution of the iron oxide particles, as well as their deposition and detachment pattern on the membrane surface [22].

Since fouling has a significant impact on the permeate quality and quantity, pretreatment of water for the removal of potential foulant is crucial to ensure consistent high-quality water production from the operation of RO and NF membranes [24,25]. The rapid fouling of all the membranes, especially the high-pressure membranes (NF and RO), suggests that the CE requires prefiltration to maintain stable and constant operation, as well as to obtain higher membrane flux rates.

From the initial screening experiments, the following conclusions can be made:

- The permeate quality and quantity were dependent upon the tested membrane type and applied operating pressure. Both MF and UF produced effluent concentrations below 1.3 ng Hg/L

at pressures  $\geq 2.8 \text{ bar}$ . The RO and NF membranes operating at 20.7 bar also provided effluent mercury concentrations of  $<1.3 \text{ ng/L}$ . The increase in the operating pressure resulted in an increase in the permeate mercury concentration.

- The sharp decrease in permeate flux (55–85% reduction in initial flux) after 1–3 h of operation was presumably due to a rapid build-up of solids on the membrane surface.
- Focused experiments were then performed only on MF/UF due to following reasons: (a) They successfully achieved the target limits at a lower operating pressure which is very attractive for reducing capital and operation costs, and (b) NF/RO membranes did not appear to add substantial benefits, given that their operation usually requires wastewater pretreatment using MF or UF membranes [18].

### 3.2. Focused testing

Since the higher solids concentration was the primary cause for the membrane fouling during the operation, focused tests were performed by operating the membrane filters sequentially to maintain stable permeate flow, low operating pressure and less membrane fouling, as shown in Fig. 3. Experiments were performed with approximately 34 L of CE, which were filtered through 5  $\mu\text{m}$ , then 1  $\mu\text{m}$  and 0.45  $\mu\text{m}$ , in-line capsule microfilters to reduce the fouling of the membranes [28,29]. The characteristics of the initial CE and the CE filtered through in-line filters are summarized in Fig. 4. The permeate from the 0.45  $\mu\text{m}$  filter was used to feed the MF unit.

The MF unit was operated at 2.8 bar pressure. The permeate from the MF unit was collected and used to feed the UF unit. The UF filtration experiments were performed with two different operating pressures: 3.4 and 6.9 bar. Fig. 4 also shows the influent and effluent characteristics, as well the performance summary for the MF and UF membranes. The percentage of mercury removal, as well as the particle removal abilities of the membranes (Fig. 6) provided the basis for the membrane performance comparison. Both membranes demonstrated excellent mercury removal ( $<0.5 \text{ ng/L}$ ).

The permeate from 0.3  $\mu\text{m}$  MF was also spiked with 20 ng Hg/L (soluble/ionic Hg in 5%  $\text{HNO}_3$ , Spex Certi Prep, New Jersey) to investigate the removal of soluble Hg with UF as well. The overall percentage of Hg removal was 69%. This result might be due to the complexation of soluble mercury ions with colloidal particles existing in the wastewater. To bring mercury concentrations to 1.3 ng/L in the presence of soluble mercury, other technologies such as precipitation, carbon adsorption or RO and NF membranes may be combined with filtration, to remove the dissolved mercury. Understanding the chemical form and species of the mercury in the untreated wastewater is crucial in technology selection [7].

It was observed that flux rates increased significantly after prefiltration of the CE (Microfiltration<sub>t=0</sub>: 232 L/(m<sup>2</sup> h) and Ultrafiltration<sub>t=0</sub>: 187 L/(m<sup>2</sup> h)). Differences in the fouling rates of

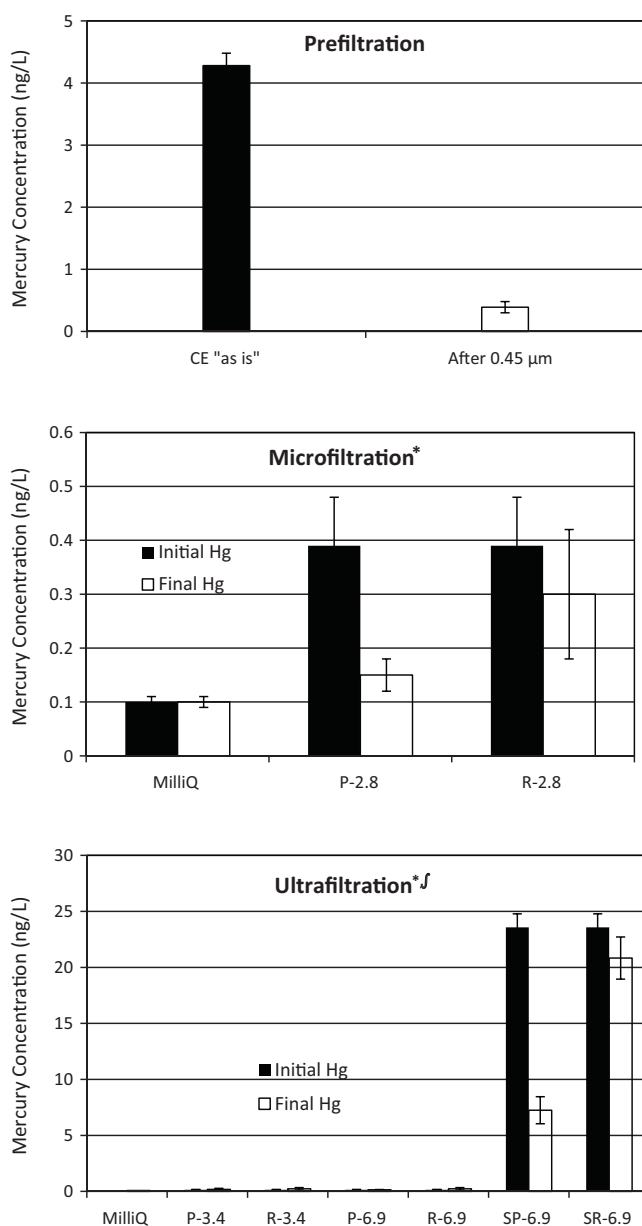


**Fig. 4.** Inlet and effluent characteristics and performance summary for prefiltration, microfiltration (averages of five replicates) and ultrafiltration (averages of triplicate samples). \*P: Permeate at specified pressure (bar). \*R: Retentate at specified pressure (bar). <sup>J</sup>SP: Permeate at specified pressure (bar) taken from spiked CE samples. <sup>J</sup>SR: Retentate at specified pressure (bar) taken from spiked CE samples.

the MF and UF, with and without prefiltration, can be shown in the differences in  $t_0$  fluxes (Table 3), as well as in the decrease in flux rates (Fig. 5). Using MF as a pretreatment would enhance UF performance by increasing the removal of particulates, which in turn would produce a significant increase in the flux rates (Table 3 and Fig. 5). The UF flux slightly decreased over the period that was studied. However, the flux reduction was higher with MF. The permeate flux decline was 66% with MF and 32% with UF at the end of the experiments. The steady decrease in the flux rates of MF could be attributed to the membrane unit, with the 42 cm<sup>2</sup> filter area having reached its performance limit after filtering 34 L of prefiltered CE, or to foulants that remained in the prefiltered CE. These results also suggest the possibility of potentially different fouling mechanisms, since the chemistry of the membrane materials was not the same.

Conclusions from the focused tests are as follows:

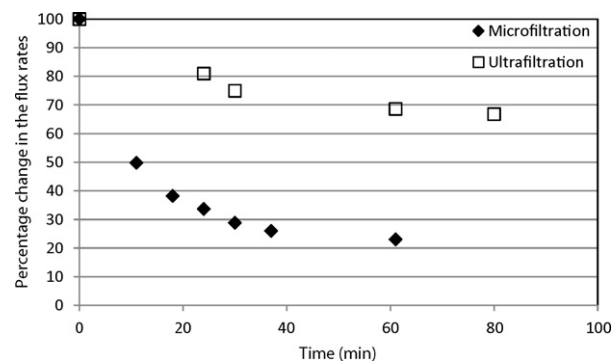


**Fig. 5.** Changes in the permeate flux rates with the operating time.

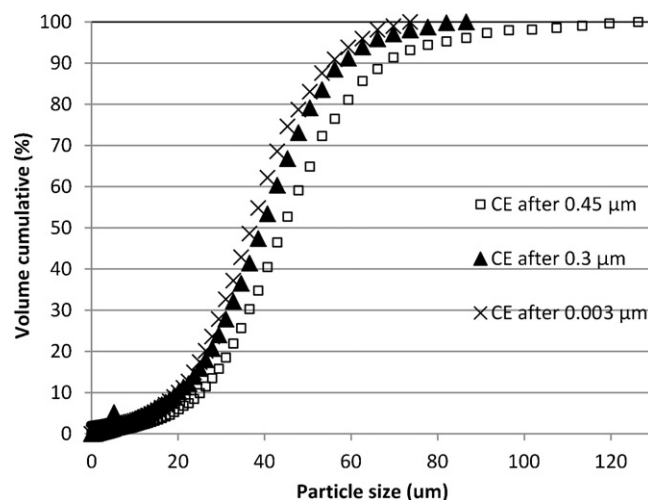


**Fig. 6.** Cumulative percentage frequency particle size distributions between membrane filtration processes.

- Sequential operation of membrane filtration units resulted in high permeate flow rates and stable low operating pressures.
- Both MF and UF confirmed the capability to achieve <1.3 ng Hg/L concentration under operating pressures  $\geq 2.8$  bars. Also, 91% of the mercury was removed after 0.45  $\mu\text{m}$  filtration, and 96% of the mercury was removed after 0.3  $\mu\text{m}$  filtration.

### 3.3. Particle size and size distribution analysis

The correlation between mercury concentration and particle size distribution was also investigated in this study to obtain a better understanding of mercury removal mechanisms by membrane filtration technologies. A particle size distribution analysis was conducted by using the Accusizer 770 (Worcestershire, UK) with an MDL of 0.5  $\mu\text{m}$ , which works on the principle of light obscuration. The test results were presented both as number and volume distributions based on the average of three measurements. As shown in Table 4, the mean particle size decreased with filtration. The mean particle size of the CE "as-is" samples was  $1.1 \pm 0.0 \mu\text{m}$ , decreasing to  $0.74 \pm 0.2 \mu\text{m}$  after UF. Table 4 also shows that 90% of the particles contained in the CE "as-is" samples were below 1.2  $\mu\text{m}$ , while 90% of the particles were less than 0.85  $\mu\text{m}$  after UF. Less than 10% of the particles in all of the tested samples were below 0.54  $\mu\text{m}$ . This indicates that the membranes with a  $\leq 0.45 \mu\text{m}$  cut-off pore size can reject more than 90% of the particles contained in the samples. A further reduction in the particle size distribution was noticed after MF and UF, as shown in Fig. 6. The size and frequency of the particles decreased after the MF process and again after the UF process.

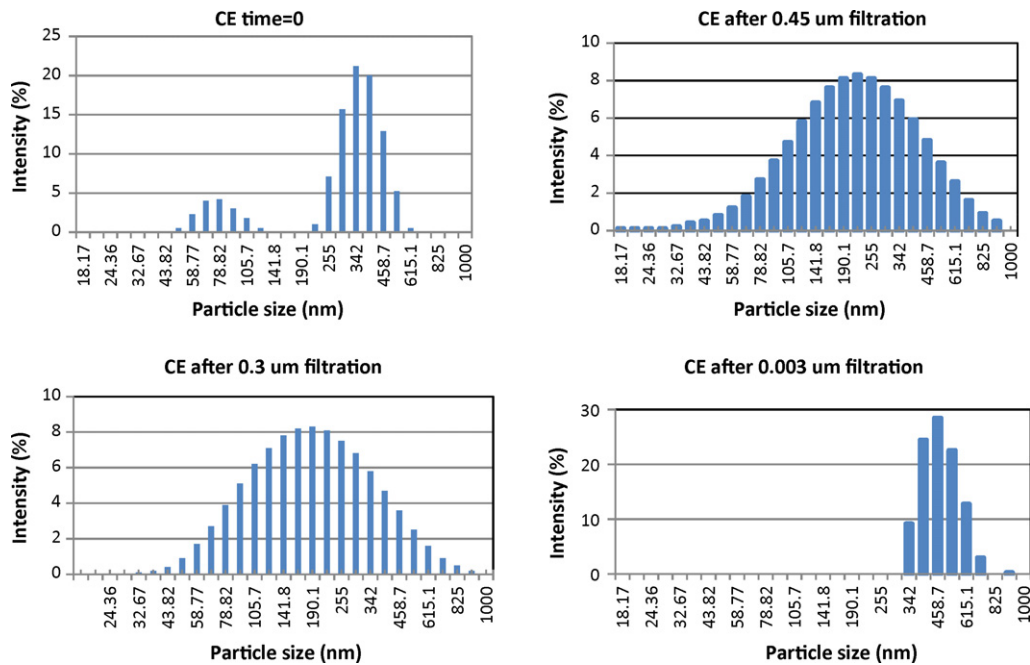


Fig. 7. Particle size distribution of CE samples analyzed with Malvern Zetasizer Nano.

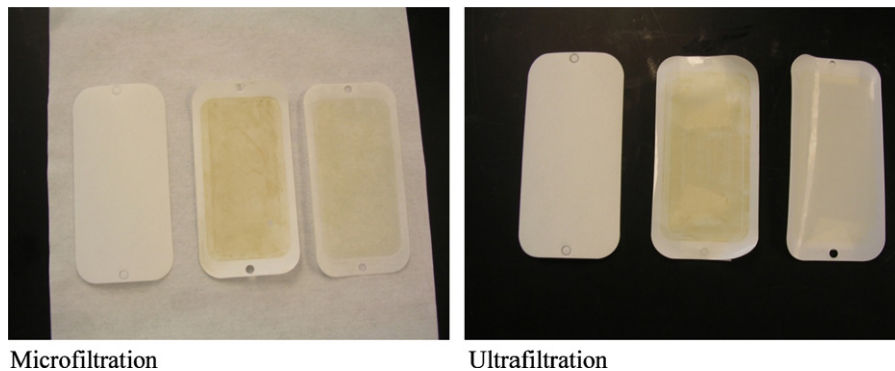


Fig. 8. Fouling of membrane filters.

Table 5

Average particle diameter size for particles less than 1  $\mu\text{m}$  by Zetasizer.

Sample	Average diameter (nm)
CE as-is	570
CE after 0.45 $\mu\text{m}$	185
CE after 0.3 $\mu\text{m}$	170
CE after 0.003 $\mu\text{m}$	Not applicable

The refinery's historic particle size analysis (PSA) data support our findings, since more than 90% of the particles in the CE were larger than 0.54  $\mu\text{m}$ , based on PSA [7]. These findings were also consistent with Dean and Mason's (2009) findings [4].

The same samples also were analyzed with the photon correlation spectroscopy/dynamic light scattering technique (Malvern Zetasizer Nano, with MDL of 0.4 nm) to determine the size distribution of the submicron particles. Fig. 7 shows that the CE "as-is" samples had a wide particle size distribution range, but after filtration this range became narrower. There were a couple of very large particles present in the samples after 0.003  $\mu\text{m}$  filtration. The mean particle diameter of submicron particles also decreased with filtration from 570 nm to 170 nm after MF, as shown in Table 5. The mean particle size for the samples filtered through 0.003  $\mu\text{m}$  membranes could not be determined, since the samples included only

a few very large particles. Because of their size, they have skewed the average diameter calculations.

#### 3.4. Membrane characteristics and morphology

Fig. 8 shows the clear advantage of using sequential filtration over no pretreatment. Prefiltration prior to MF and the subsequent use of permeate from MF into UF resulted in considerably higher flux rates and lower fouling of these membranes while the mercury removal performance of UF was unchanged. As depicted in the photos, the color of the deposition layer on the membrane surfaces was lighter in the prefiltered tests than in the tests with no prefiltration.

SEM analysis was used to compare surface morphology of clean and fouled membranes. The SEM analysis demonstrated that pore blockage and narrowing were the dominant fouling mechanisms for MF membrane (0.3  $\mu\text{m}$ ) (Fig. 9). Pore size was reduced or blocked by adsorption or retention of particles. The SEM images of clean and fouled MF membranes show that the deposition of particles on the membrane appeared to constrict the pore openings. This might be due to the interaction of the particles with the membrane. However, surface coverage was the dominant fouling mechanism with UF, NF and RO membranes.

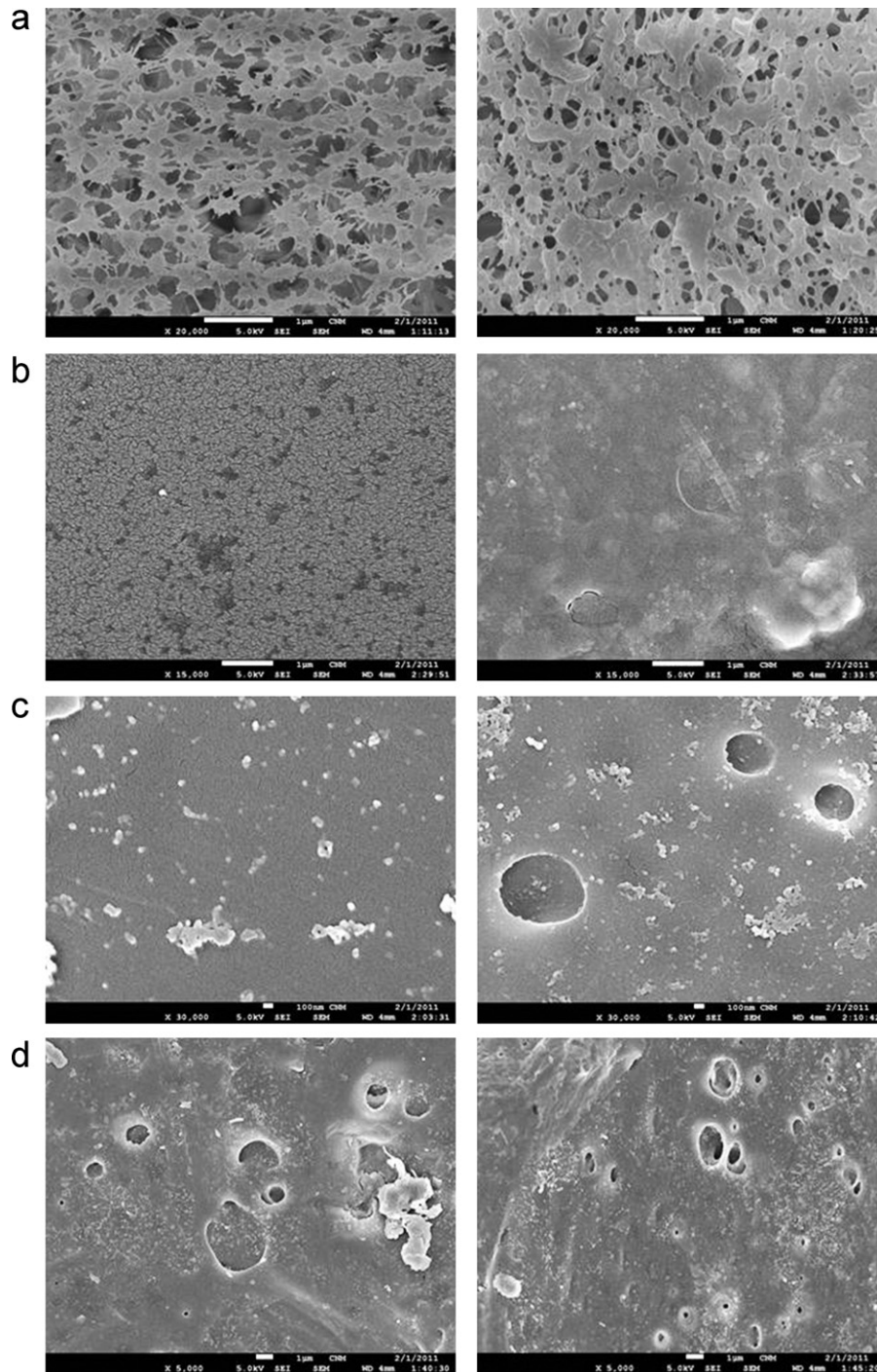


**Fig. 9.** Scanning electron micrographs of membrane filters: Left side—clean membranes; Right Side—fouled membranes: (a) Microfiltration; (b) Ultrafiltration; (c) Nanofiltration; (d) Reverse Osmosis.

Similar test results were also reported by Lee et al. [30]. MF showed more fouling than UF membrane filtration since the dominant fouling mechanism with MF was pore blockage versus surface coverage.

PSA test results (Table 5) show that the vast majority of particles (>90%) are greater than  $0.54\ \mu\text{m}$  pore size. However, less than 10% of the particles are smaller than  $0.3\ \mu\text{m}$  size. It has been reported that a small portion of the total natural organic matter (NOM) which are fractional components of NOM are responsible for the significant flux decline through reversible fouling [30].

### 3.5. Mass balance calculations

Total Hg concentration on the membrane surface was directly measured by Method 1631E [9] as described earlier. Table 6 shows the Hg concentrations of the clean and used membrane filters. The mercury content of clean membranes was subtracted from the mercury content of used membranes. The higher Hg concentrations at the MF membrane showed that mercury adsorbed onto the membrane surface as expected. Table 6 also shows the measured Hg concentration and volume of each stream.

**Table 6**  
Experimental data for mass balance calculations.

Membrane	Hg on filter		Influent		Permeate		Retentate	
	Clean (ng/filter)	Used (ng/filter)	Hg (ng/L)	Volume (L)	Hg (ng/L)	Volume (L)	Hg (ng/L)	Volume (L)
MF	0.55	19.2	5.96	18.925	0.55	2.5	5.69	16.425
UF	1.27	1.93	0.15	18.925	0.14	17.925	0.23	1.0

The Hg mass balance can be written as follows:

#### 1. Wastewater volume

$$V_{\text{inf}} = V_{\text{per}} + V_{\text{ret}} \quad (1)$$

#### 2. Convert the given constituent quantities in Table 6 to mass values:

$$C_{\text{inf}} \times V_{\text{inf}} = C_{\text{per}} \times V_{\text{per}} + C_{\text{ret}} \times V_{\text{ret}} + \text{Hg}_{\text{filter}} \quad (2)$$

Hg mass balance for MF

$$5.96 \text{ ng Hg/L} \times 18.925 \text{ L} \cong 0.55 \text{ ng Hg/L} \times 2.5 \text{ L} + 5.69 \text{ ng Hg/L} \\ \times 16.425 \text{ L} + 18.65 \text{ ng}$$

$$112.8 \text{ ng Hg} \cong 113.5 \text{ ng Hg}$$

This calculation demonstrates that the total mercury content was essentially the same (within 0.6%) before and after the operation of the microfiltration membrane unit. Given that the equipment and method blanks show that there is no mercury loss or contamination during the operation of membrane unit, the mass conservation of Hg within the membrane system is confirmed. This calculation also shows that more than 16% of the Hg in the influent was adsorbed onto the membrane surface after 1 h of membrane operation.

Hg mass balance for UF

$$0.15 \text{ ng Hg/L} \times 18.925 \text{ L} \approx 0.14 \text{ ng Hg/L} \times 17.925 \text{ L} + 0.23 \text{ ng Hg/L} \\ \times 1.0 \text{ L} + 0.66 \text{ ng}$$

$$2.84 \text{ ng Hg} \approx 3.40 \text{ ng Hg}$$

The mercury detected on the UF membrane was low (0.66 ng/L) since the experiments were performed with wastewater containing very low mercury concentrations (0.15 ng/L). The difference between input and output mercury content (about 19%) might be due to analytical errors when measuring very low ng/L concentrations by Method 1631E with MDL of 0.5 ng/L in most cases [9].

## 4. Conclusions

This study provides a bench-scale evaluation of membrane technologies in achieving the world's most stringent Hg discharge limits with refinery wastewater. The major findings from this study are:

- The experimental test results indicated that MF and UF membranes with operating pressure of  $\geq 2.8$  bar were highly effective in removing mercury, which was present mostly in particulate form. The water quality goal of  $<1.3$  ng Hg/L was met and exceeded after MF and UF membrane processes.
- Both NF and RO were also able to meet the target mercury concentration when operated at lower pressures (20.7 bar). However, The RO and NF membranes with no pretreatment were unable to remove particulate mercury completely from the refinery wastewater at higher operating pressures ( $\geq 34.5$  bar). This result might be due to concentration polarization because of solids deposition on the membrane surface or due to breakage of particulate bond Hg under high convective flow, followed by

release into the permeate, and hence decrease in the rejection of Hg.

- The correlation between mercury concentration and particle size distribution indicates that the membranes with a  $\leq 0.45$   $\mu\text{m}$  cut-off pore size can reject more than 90% of the particles contained in the refinery samples and can also meet the target Hg concentration ( $<1.3$  ng/L). A further reduction in the particle size distribution and frequency of the particles as well as Hg concentration in the treated wastewater was found after MF and UF treatment.
- A series of analyses, including SEM and optical observation, flux and Hg rejection measurements confirmed that the membranes were fouled by the refinery wastewater. The SEM images and pictures of membranes indicate the build-up of the fouling layer on the membrane surfaces after exposure to the refinery wastewater. The sharp decrease in permeate fluxes (55–85% of initial fluxes) after 1–3 h of operation is due to a rapid build-up of a fouling layer on the membrane surfaces. Although the product recovery percentages of each tested membrane initially increased with the increasing operating pressures, the membranes fouled more severely in a short period of operation time as higher convective flow results in increased deposition of solids on the membrane surface.
- The mass balance calculations for Hg showed that total mercury content was the same before and after the operation of MF unit, and confirmed the accumulation of Hg within the membrane system.
- Pilot-scale studies are needed to determine the flux and rejection properties of the tested membranes systematically and to confirm the mercury removal performance of MF and UF membranes under continuous and varying influent conditions.

## Acknowledgements

This work was sponsored via Purdue University by BP Products North America Inc. through Agreement No. 85V09 with the University of Chicago Argonne LLC.

## References

- [1] U.S. Environmental Protection Agency, National Recommended Water Quality Criteria-Priority Pollutants, 2011 (accessed 31.05.11) <http://water.epa.gov/scitech/swguidance/standards/current/index.cfm#appendxa>.
- [2] U.S. Environmental Protection Agency, Mercury Study Report to Congress, Office of Air Quality Planning and Standards; Office of Research and Development, EPA/452/R-976/003, Washington, DC, 1997, December (accessed 31.05.11) <http://www.epa.gov/ttn/atw/112nmerc/volume1.pdf>.
- [3] Water Quality Guidance for the Great Lakes System: Supplementary Information Document (SID), United States Environmental Protection Agency Office of Water, EPA-820-B-95-001, 1995, March.
- [4] J.D. Dean, R.P. Mason, Estimation of Mercury Bioaccumulation Potential from Wastewater Treatment Plants in Receiving Waters: Phase I Final Report, Water Environment Federation Report 05-WEM-10C, Water Environment Federation, Alexandria, Virginia, 2009.
- [5] Sterlitech CF042 Cell, 2011 (accessed 5.11.11) [www.sterlitech.com](http://www.sterlitech.com).
- [6] R.A. Bertelsen, D.L. Olsen, Cross-flow filtration membrane test unit, U.S. Patent 4,846,970 (1989).
- [7] M.C. Negri, P.S. Gillenwater, M. Urgan-Demirtas, Emerging Technologies and Approaches to Minimize Discharges into Lake Michigan. Phase 2, Module 3 Report, ANL-11/13 Argonne National Laboratory, Lemont, IL, 2011 (Peer Reviewed).
- [8] US EPA Method 1669, Sampling Ambient Water for Trace Metals at EPA Water Quality Criteria Levels, 1996, July.

- [9] US EPA Method 1631, Revision E, Mercury in Water by Oxidation, Purge and Trap, and Cold Vapor Atomic Fluorescence Spectrometry, 2002, August.
- [10] S. Norouzbahari, R. Roostaazad, M. Hesampour, Crude oil desalter effluent treatment by a hybrid UF/RO membrane separation process, *Desalination* 238 (2009) 174–182.
- [11] S. Bouranene, P. Fievet, A. Szymczyk, M. El-Hadi Samer, A. Vodonne, Influence of operating conditions on the rejection of cobalt and lead ions in aqueous solutions by a nanofiltration polyamide membrane, *J. Membr. Sci.* 325 (2008) 150–157.
- [12] C.J. Harrison, A.E. Childress, Y.A. Le Goullec, R.C. Cheng, Bench-scale testing of seawater desalination using nanofiltration, in: *AWWA, Membrane Technology Conference*, 2005.
- [13] Metcalf & Eddy, *Wastewater Engineering*, 4th ed., Mc Graw Hill, 2003.
- [14] N. Hilal, G. Busca, N. Hankins, A.W. Mohammad, The use of ultrafiltration and nanofiltration membranes in the treatment of metal-working fluids, *Desalination* 167 (2004) 227–238.
- [15] A.W. Mohammad, R. Othaman, N. Hilal, Potential use of nanofiltration membranes in treatment of industrial wastewater from Ni-Pd electroless plating, *Desalination* 168 (2004) 241–252.
- [16] M.C.V. Soares, M.A. Bertrams, F.A. Lemos, I.O.C. Masson, Removal of lead, cadmium and zinc from industrial effluents using nanofiltration and reverse osmosis membranes, in: *XIII International Conference on Heavy Metals in the Environment*, Rio de Janeiro, Brazil, 2005.
- [17] *Standard Methods for the Examination of Water and Wastewater*, SM 2560D, 21st ed., APHA/AWWA/WEF, 2005.
- [18] J-S. Choi, T-M. Hwang, S. Lee, S. Hong, A systematic approach to determine the fouling index for a RO/NF membrane process, *Desalination* 238 (2009) 117–127.
- [19] B.A. Winfield, A study of the factors affecting the rate of fouling of reverse osmosis membranes treating secondary sewage effluents, *Water Res.* 13 (1979) 565–569.
- [20] A.I. Schafer, U. Schwicker, M.M. Fischer, A.G. Fane, T.D. Waite, Microfiltration of colloids and natural organic matter, *J. Membr. Sci.* 330 (2009) 90–103.
- [21] D.C. Sioutopoulos, S.G. Yiantsios, A.J. Karabelas, Relation between fouling characteristics of RO and UF membranes in experiments with colloidal organic and inorganic species, *J. Membr. Sci.* 330 (2010) 62–82.
- [22] X. Zhu, M. Elimelech, Colloidal fouling of reverse osmosis membranes: measurements and fouling mechanisms, *Environ. Sci. Technol.* 31 (1997) 3654–3662.
- [23] T. Shibutani, T. Kitaura, Y. Ohmukai, T. Maruyama, S. Nakatsuka, T. Watabe, T. Matsuyama, Membrane fouling properties of hollow fiber membranes prepared from cellulose acetate derivatives, *J. Membr. Sci.* 376 (2011) 102–109.
- [24] K.O. Agenson, T. Urase, Change in membrane performance due to organic fouling in nanofiltration (NF)/reverse osmosis (RO) applications, *Sep. Purif. Technol.* 55 (2007) 147–156.
- [25] H.Y. Ng, M. Elimelech, Influence of colloidal fouling on rejection of trace organic contaminants by reverse osmosis, *J. Membr. Sci.* 244 (2004) 215–226.
- [26] A.E. Contreras, A. Kim, Q. Li, Combined fouling of nanofiltration membranes: mechanisms and effect of organic matter, *J. Membr. Sci.* 327 (2009) 87–95.
- [27] A.R.D. Verliefde, E.R. Cornelissen, S.G.J. Heijman, I. Petrinic, T. Luxbacher, G.L. Amy, B. Van der Bruggen, J.C. van Dijk, Influence of membrane fouling by (pretreated) surface water on rejection of pharmaceutically active compounds (PhACs) by nanofiltration membranes, *J. Membr. Sci.* 330 (2009) 90–103.
- [28] R. Fabris, E.K. Lee, C.W.K. Chow, V. Chen, M. Drikas, Pre-treatments to reduce fouling of low pressure microfiltration (MF) membranes, *J. Membr. Sci.* 289 (2007) 231–240.
- [29] J. Kim, W. Shi, Y. Yuan, M.B. Benjamin, A serial investigation of membrane fouling by natural organic matter, *J. Membr. Sci.* 294 (2007) 115–126.
- [30] N. Lee, G. Amy, J-P. Croue, H. Buisson, Morphological analyses of natural organic matter (NOM) fouling of-pressure membranes (MF/UF), *J. Membr. Sci.* 261 (2005) 7–16.